Boundary Layers Associated with Thermally Forced Planetary Waves

R. S. LINDZEN AND J. M. FORBES

Center for Earth and Planetary Physics, Harvard University, Cambridge, MA 02138

(Manuscript received 24 January 1978, in final form 4 April 1978)

ABSTRACT

We examine the boundary layers associated with thermally forced waves in a viscous, stably stratified, rotating, spherical atmosphere. Forcing is in the form of inviscid Hough modes corresponding to gravity and Rossby waves having critical latitudes. The response does not, in general, have the same meridional form as the forcing. Although the boundary layer response is rather complicated, it can be said that the critical latitudes are not, in general, the locus of significantly enhanced boundary layer convergence. The primary source of boundary layer convergence is associated with conventional Ekman pumping in Rossby waves. There can be locally enhanced convergence for gravity waves, but such convergence is always associated with that part of the response orthogonal to the forced mode.

1. Introduction

The character of frictional boundary layers for tropical flows has been of interest for some time. It was noted by Greenspan (1968) that for oscillations in a spherically contained, viscous, rotating, homogeneous, incompressible fluid, the boundary layer pumping "blew up" at critical latitudes where the oscillatory frequency equaled the local Coriolis frequency. In the case of steady motions, this latitude is the equator. A number of studies have attempted to show that similar singular boundary layer pumping should occur for a stratified atmosphere (Charney, 1971; Holton *et al.*, 1971; Yamasaki, 1971). These studies, however, were defective in that they did not properly allow for interactions between boundary layer and interior flows—in particular the role of stratification in permitting modifications of boundary layer pressures was ignored. For steady flows, Kuo (1973) and Schneider and Lindzen (1976) showed that such interactions effectively eliminated singular boundary layer behavior at the equator.

The purpose of the present paper is to similarly examine boundary layers for thermally forced waves. As has been noted, the existence of singular (or pronounced but non-singular) boundary layer pumping at critical latitudes could have significant implications for the existence of the ITCZ (intertropical convergence zone) (Holton *et al.*, 1971). More generally, it is believed that many tropical disturbances are thermally forced by latent heat release in cumulonimbus towers, and that the cumulonimbus towers themselves respond to the convergence of moisture in the boundary layer of the disturbance. This collective interaction of cumulus convection and larger scale disturbances is known as CISK (conditional instability of the second kind) and was first discussed in connection with hurricanes by Charney and Eliassen (1964). The role of a CISK mechanism in tropical waves has also been examined (Hayashi, 1970; Lindzen, 1974, and many others); in the case of internal waves, there can be low-level convergence in the absence of friction. However, in all cases the role of friction in contributing to low-level convergence is potentially very important. Indeed, Holton (1975), investigating the convergence forced in a vertically integrated boundary layer of fixed thickness by a prespecified pressure distribution corresponding to an inviscid mixed gravity-Rossby mode, concluded that boundary layer convergence greatly exceeded inviscid wave convergence for all but very long zonal scales, and that maximum boundary layer convergence occurred near the critical latitude. Holton, however, once again did not allow the boundary layer to dynamically affect the interior dynamics.

Shapiro (1977), considering Rossby waves on a midlatitude β-plane, showed that the consistent coupling of interior and boundary solutions (in contrast to the arbitrary imposition of the interior solution) considerably reduced the boundary layer convergence predicted by Holton's procedure. Shapiro employed a midlatitude β-plane geometry because the equations with friction remain separable with respect to height and latitude dependence in such a geometry; friction eliminates separability on a sphere and for an equatorial β-plane.[1] Unfortunately, on a midlatitude β-plane there is no critical latitude, so Shapiro could not determine

[1] In this respect, as well, Holton's imposition of a single interior mode is inconsistent.

0022-4928/78/1441-1449$05.00
© 1978 American Meteorological Society

whether Holton's conclusions vis-à-vis enhanced pumping at such a latitude were reasonable.

The purpose of the present paper is to consistently examine the boundary layer associated with thermally forced waves in a stratified, compressible, viscous gas on a rotating sphere. Because of the inseparability of the relevant equations, our approach is, of necessity, numerical. Relatedly, although we shall assume thermal forcing to have the meridional shape of specific inviscid spherical wave modes (corresponding to gravity waves, mixed gravity-Rossby waves and Rossby waves—all with critical latitudes) our calculated response will not, in general, have the same shape. Because of the length of suitably accurate numerical computations, only a limited number of cases could be run. However, care was taken that these cases be representative.

The details of our equations, numerical methods and boundary conditions are described in Sections 2 and 3. A brief discussion of the various wave modes studied is given in Section 4, while our boundary layer results are presented in Section 5. Conclusions are described in Section 6.

Briefly, we find no special boundary layer pumping at critical latitudes. Moreover, if we decompose wave response into projections on the forced mode and on other orthogonal modes, we find enhanced boundary layer convergence for the former only for Rossby waves and mixed gravity-Rossby waves which are of a distinct Rossby character. Such enhanced pumping as is present for gravity waves is exclusively associated with mode coupling into modes other than the one which was directly forced.

2. Governing equations and method of solution

The system of equations assumed to govern the thermally forced planetary wave and boundary layer dynamics consists of the linearized momentum, continuity and thermal energy perturbation equations for a rotating, spherical, viscous atmosphere, where the (unperturbed) state is assumed motionless and a function of height only:

$$\frac{\partial u'}{\partial t}+2\Omega\cos\theta v'=-\frac{1}{a\sin\theta}\frac{\partial\Phi'}{\partial\lambda}+\frac{1}{\rho_0}F_\lambda, \tag{1}$$

$$\frac{\partial v'}{\partial t}-2\Omega\cos\theta u'=-\frac{1}{a}\frac{\partial\Phi'}{\partial\theta}+\frac{1}{\rho_0}F_\theta, \tag{2}$$

$$\frac{1}{a\sin\theta}\frac{\partial u'}{\partial\lambda}+\frac{1}{a\sin\theta}\frac{\partial\sin\theta v'}{\partial\theta}+\frac{\partial w^{*\prime}}{\partial x}-w^{*\prime}=0, \tag{3}$$

$$\frac{1}{R}\frac{\partial^2\Phi'}{\partial t\partial x}+\Gamma w^{*\prime}=\frac{J}{c_p}-\frac{a_c}{R}\frac{\partial\Phi'}{\partial x}, \tag{4}$$

where

θ	colatitude
λ	longitude
x	$-\ln(p/p_0)$
p	pressure
p_0	surface pressure
t	time
u'	westerly velocity
v'	northerly velocity
$w^{*\prime}$	$-(1/p)Dp/Dt$
Φ'	perturbation geopotential
R	gas constant
c_p	heat capacity at constant pressure
F_i	divergence of momentum flux in the ith direction due to diffusion
J	heating rate per unit mass
a_c	Newtonian cooling coefficient
Ω	rotation rate of earth
a	radius of earth
Γ	$\partial T/\partial x+\kappa T$
T	temperature of unperturbed atmosphere
κ	R/c_p.

Thermal conduction is neglected in the above formulation. While this decision was partially influenced by computer limitations, the essential physics and conclusions of this paper should remain unaffected. As shown in Section 3, inclusion of Newtonian cooling is merely an artifice to ensure proper upper boundary conditions. Assuming zonally propagating wave solutions of the form

$$\begin{Bmatrix}u'\\v'\\w^{*\prime}\\\Phi'\end{Bmatrix}=\begin{Bmatrix}u\\v\\w\\\Phi\end{Bmatrix}\exp[x/2+i(\omega t+s\lambda)],$$

Eqs. (1)–(4) combine to yield

$$i\omega u+2\Omega\cos\theta v=\frac{-is}{a\sin\theta}\Phi+\frac{\nu_{\text{eddy}}}{H^2}F(u), \tag{5}$$

$$i\omega v-2\Omega\cos\theta u=-\frac{1}{a}\frac{\partial\Phi}{\partial\theta}+\frac{\nu_{\text{eddy}}}{H^2}F(v), \tag{6}$$

$$\frac{\partial^2\Phi}{\partial x^2}-\left(\frac{1}{\Gamma}\frac{d\Gamma}{dx}+\frac{i}{\omega_c}\frac{da_c}{dx}\right)\frac{\partial\Phi}{\partial x}-\left(\frac{1}{4}+\frac{1}{2\Gamma}\frac{d\Gamma}{dx}+\frac{i}{2\omega_c}\frac{da_c}{dx}\right)\Phi+\frac{i\Gamma R}{\omega_c}\left(\frac{is}{a\sin\theta}u+\frac{1}{a\sin\Theta}\frac{\partial\sin\theta v}{\partial\theta}\right)=\frac{-\kappa e^{-x/2}}{i\omega_c}\left[\left(1+\frac{1}{\Gamma}\frac{d\Gamma}{dx}\right)J-\frac{dJ}{dx}\right], \tag{7}$$

where

$$\omega_c=\omega-ia_c,$$

$$F=\frac{\partial^2}{\partial x^2}+\left(\frac{1}{\nu_{\text{eddy}}}\frac{\partial\nu_{\text{eddy}}}{\partial x}-\frac{2}{H}\frac{dH}{dx}\right)\frac{\partial}{\partial x}+\left(\frac{1}{2\nu_{\text{eddy}}}\frac{\partial\nu_{\text{eddy}}}{\partial x}-\frac{1}{H}\frac{dH}{dx}-\frac{1}{4}\right),$$

and ν_{eddy} is the kinematic eddy viscosity coefficient.

The eddy diffusion coefficient is chosen to be equal to a constant value of 10 $m^2\ s^{-1}$ within the troposphere, and to increase exponentially above the region of thermal excitation (described later) to behave as a nonreflecting or "spongy" layer. For later reference, we noted that $w^{*\prime}$ can be computed from the solution for Φ':

$$w^{*\prime}=\frac{J}{C_p\Gamma}-\frac{i\omega_c}{\Gamma R}\frac{\partial\Phi'}{\partial x} \tag{8}$$

and that the vertical velocity (in height coordinates) is given by

$$w=\frac{i\omega}{g}-\Phi'+Hw^{*\prime}. \tag{9}$$

For an inviscid atmosphere ($\nu_{\text{eddy}}=0$), the governing equations can be further simplified. Eqs. (1)–(3) combine to give

$$\frac{\partial w^{*\prime}}{\partial x}-w^*=-\frac{i\omega}{4a^2\Omega^2}F(\Phi'), \tag{10}$$

where F is the Laplace's tidal operator (Chapman and Lindzen, 1970). Eliminating $w^{*\prime}$ between (4) and (10) yields a single equation for Φ:

$$\begin{aligned}\alpha_\theta^2\frac{\partial^2\phi}{\partial x^2}-\alpha_\theta^2\left[\frac{1}{\Gamma}\frac{d\Gamma}{dx}+\frac{i}{\omega_c}\frac{da_c}{dx}\right]\frac{\partial\Phi}{\partial x}-\beta\alpha_\theta\frac{\partial^2\Phi}{\partial\theta^2}\\ -\beta[\alpha_\theta\cot\theta-2\sin\theta\cos\theta]\frac{\partial\Phi}{\partial\theta}\\ -\left[\left(\frac{1}{4}+\frac{1}{2\Gamma}\frac{d\Gamma}{dx}+\frac{i}{2\omega_c}\frac{da_c}{dx}\right)\alpha_\theta^2\right.\\ \left.-\beta\frac{S}{\alpha}(\alpha^2+\cos^2\theta)-\beta\alpha_\theta\frac{S^2}{\sin^2\theta}\right]\Phi\\ =-\frac{\alpha_\theta^2\kappa e^{-x/2}}{i\omega_c}\left[\left(1+\frac{1}{\Gamma}\frac{d\Gamma}{dx}\right)J-\frac{dJ}{dx}\right],\end{aligned} \tag{11}$$

where

$$\left.\begin{aligned}\alpha_\theta^2&=\alpha^2-\cos^2\theta\\ \beta&=\frac{\Gamma R}{4a^2\Omega^2}\frac{\omega}{\omega_c}\\ \alpha&=\frac{\omega}{2\Omega}\end{aligned}\right\}.$$

The thermal excitation is assumed to be of the form $J=\hat{J}(x)\Theta(\theta)$, where $\Theta(\theta)$ is the Hough function for a particular mode and

$$\hat{J}=\begin{cases}0, & z>30\text{ km},\ z<5\text{ km}\\ \hat{J}_{\max}\exp\{-[(x-x)_{\max}/\Delta x]^2\}, & 5\text{ km}\leqslant z\leqslant 30\text{ km},\end{cases}$$

where $x_{\max}=2.0$ ($z\approx 15$ km), $\Delta x=0.50$ (half-width ≈ 10 km), and $\hat{J}_{\max}$ is arbitrarily chosen to be 0.05 J kg^{-1}. This vertical structure was chosen such that J is negligibly small below the altitude where dissipation becomes important (see Section 3), and such that the heat source is external to the planetary boundary layer. In the latter sense, the heat source resembles that of cumulonimbus heating in the tropics, where the heating occurs above the cumulonimbus cloud base, and hence above the mixed surface layer.

Discretizing (5)–(7) with respect to θ results in a system of $3(k-1)$ second-order ordinary differential equations in x, where k is the number of grid points in the θ-direction. The Gaussian elimination algorithm presented by Lindzen and Kuo (1969) was utilized to solve the system of ordinary differential equations. Since the modes to be simulated are of planetary scale, whereas possible critical latitude effects might occur on a shorter horizontal scale, the selection of grid points in the θ-direction was economized by transforming to a stretched horizontal variable to allow maximum resolution near θ_c, i.e.,

$$\theta'=1.50+\tan^{-1}[k(\theta-\theta_c)]+\tan^{-1}k\theta_c \tag{12}$$

so that $\delta\theta=\{1.5+k/[1+k^2(\theta-\theta_c)^2]\}^{-1}\delta\theta'$. Numerical simulations were performed for various values of k to ensure that any anomalous features of the boundary layer related to the critical latitude occurred on a scale much larger than the finite difference grid. A choice of $k=8$ and $\delta\theta'=10.5°$ proved adequate, and the corresponding finite-difference grid spacing are indicated in Figs. 6–10 for five of the modes. As it turns out, numerical solutions using a constant $\delta\theta=3.75°$ (no stretching) resulted in little difference from the results using a stretched finite difference grid.

Similarly, a stretched vertical coordinate was implemented to allow better height resolution within the boundary layer, i.e.,

$$x'=a[1-b/(x+b)]+x, \tag{13}$$

so that $\delta x=[1+ab/(x+b)^2]^{-1}\delta x'$. Values of $a=4.0$ and $b=0.25$ yielded 20 grid points below 1 km, 32 points below 2 km and 49 points below 5 km.

Eq. (11) can be solved by separation of variables, where the θ-dependence is governed by the Laplace tidal equation (Hough functions), or by the direct numerical integration used to solve (5)–(7). We found it useful to utilize the separable solution to check the numerical integration scheme. For instance, by assuming $\Phi=\phi(x)\Theta(\theta)$ and $F(\theta)=(-4a^2\Omega^2/gh_n)\Theta$, where $\Theta(\theta)$ is the Hough function defining the horizontal structure of the excitation and h_n is the corresponding equivalent depth, an equation governing the vertical structure of Φ, $\phi(x)$ was obtained. By comparing the solutions for $\phi(x)$ with the vertical structures obtained from direct integration of (11), it was possible to verify that the x, θ integration scheme was sufficiently accurate.

TABLE 1. Wave modes.

Mode	Type	ϵ	Vertical wavelength λ_z	Zonal wavenumber s	Period T (days)	Critical latitude θ_c
I	Gravity	1.37×10^2	53.1	1	1.00	30.0°
II	Rossby-gravity ("gravity-type")	10^3	17.2	1	3.06	8.4°
III	Rossby-gravity ("gravity-type")	10^2	62.4	1	1.85	15.8°
IV	Rossby-gravity ("gravity-type")	10^3	17.2	4	4.00	7.2°
V	Rossby-gravity ("Rossby-type")	10^2	62.4	4	2.94	9.9°
VI	Rossby	10^2	62.4	4	5.88	4.9°

3. Boundary conditions

a. *Upper boundary*

The horizontal structure of the thermal excitation is assumed to follow the Hough mode shape of the particular gravity, mixed Rossby-gravity or Rossby mode under investigation. However, since the governing equations are inseparable in the presence of friction, the atmospheric response does not consist of a single mode. The upper boundary condition was therefore handled by letting the Newtonian cooling and eddy diffusion coefficients increase exponentially upward with a vertical scale such that those dissipative effects were negligible in the boundary layer and region of heating, but become dominant above the heating region, thus acting as a nonreflecting or "spongy" layer. We consider dissipation to become important when the time scale for dissipation is on the order of the wave period. Thus by defining $\chi=(4\pi^2/\lambda_z^2)\nu_{\text{eddy}}/\omega$ for the case of eddy diffusion and $\chi=a_c/\omega$ for Newtonian cooling, the level where dissipation becomes important occurs when $\chi=1$. The corresponding reflectivity is approximated by $e^{-\pi\beta}$, where $\beta=2\pi H'/\lambda_z$ and H' is the scale height for dissipation (Lindzen, 1970). We chose ν_{eddy}, a_c and H' such that $\chi=1$ occurred above the region of thermal excitation, and that $e^{-\pi\beta}\ll1$ for the range of vertical wavelengths under consideration. The corresponding boundary conditions are

$$\frac{\partial u'}{\partial x}=\frac{\partial v'}{\partial x}=\frac{\partial \Phi'}{\partial x}=0 \quad \text{at} \quad x=x_{\text{top}}. \tag{14}$$

The only difficulty with this approach is that the dissipative scale height must be kept sufficiently large to prevent reflection, thus requiring a domain of integration which is computationally inefficient (x_{top} had to be greater than about 12.0). As discussed in Section 2, this computational inefficiency was offset to a large extent by using a stretched coordinate which resulted in a fine numerical grid in the lower troposphere, and a coarser grid in the region of heating and above.

b. *Lower boundary*

The lower boundary condition on Φ' for both the inviscid and viscid models is determined from the condition that $w(0)=0$, which implies from (9) that $w^*(0)=[-i\omega/gH(0)]\Phi'$. Substituting this expression for $w^*(0)$ into (4) gives the lower boundary condition on Φ

$$\frac{d\Phi'}{dx}-\frac{\Gamma}{T}\frac{\omega}{\omega_c}\Phi'=0 \quad \text{at} \quad x=0. \tag{15}$$

The lower boundary conditions on u' and v' for a viscid atmosphere are (cf., Lindzen, 1970)

$$\frac{d}{dx}\begin{Bmatrix}u'\\v'\end{Bmatrix}-HC_s\begin{Bmatrix}u'\\v'\end{Bmatrix}=0 \quad \text{at} \quad x=0, \tag{16}$$

where $C_s=C_D|u_0|/\nu_{\text{eddy}}$ and $C_D|u_0|\approx2$ cm s^{-1}. In all our simulations $\nu_{\text{eddy}}(0)=10$ m^2 s^{-1}, so that $C_s=2\times10^{-3}$ m^{-1}.

4. Wave modes

Several wave types covering a range of naturally occurring periods and vertical scales were selected for evaluation, and are described by the data in Table 1 and Figs. 1 and 2. As in Longuet-Higgins (1968), we utilized the nondimensional parameter $\epsilon=4\Omega^2a^2/gh_n$ in defining the dispersion relations, where Ω is the planetary rotation rate, a the planetary radius, g acceleration due to gravity and h_n the equivalent depth. Vertical wavelengths were computed from

$$\lambda_z=2\pi\left[\frac{H}{h_n}\left(\kappa+\frac{1}{T}\frac{dT}{dx}\right)-\frac{1}{4}\right]^{-\frac{1}{2}}, \tag{17}$$

where H is the scale height, $\kappa=R/c_p\approx0.286$, with a tropospheric lapse rate of $-6.5°$ K km^{-1} and ground temperature = 290 K [the background temperature profile was identical to that used by Lindzen (1970) below 100 km]. The six modes listed in Table 1, consisting of one gravity, four mixed Rossby-gravity and one Rossby mode, describe the thermal forcings used in the numerical simulations. Mode I is the first symmetric propagating diurnal tidal mode (Chapman and Lindzen, 1970). As indicated by the dispersion curves in Figs. 1 and 2, the mixed Rossby-gravity waves become more Rossby-type for a given ϵ as the zonal wavenumber becomes larger. Thus modes II, III and IV can be

considered gravity-type, while mode V is Rossby-type. Mode VI is a pure Rossby mode. Note also that modes II and IV correspond to $\epsilon=10^3$ ($\lambda_z\approx17$ km), whereas the others correspond to $\epsilon\approx10^2$ ($\lambda_z\approx62$ km). Wave periods range between 5.88 and 1.00 days, which correspond to critical latitudes between 4.9° and 30.0°, respectively.

5. Results

In conventional boundary layer analyses one may, by definition as it were, unambiguously distinguish between boundary layer effects and interior solutions. As we have noted in Section 1, however, conventional analyses of the present problem have thus far been found inadequate. Our present approach has made no *a priori* attempt to distinguish a boundary layer from the interior; rather, we have solved the full set of equations at all levels, thus guaranteeing the complete self-consistency of our solutions. The solutions which emerge do exhibit boundary layer characteristics; however, because of the inseparability of the system among other things, the description of the solutions is somewhat complicated.

In Fig. 3 and 4 we show the height distribution of the amplitude of the northerly velocity component at various latitudes for two antisymmetric gravity-type mixed modes, and the height distribution of the westerly velocity amplitude at various latitudes for the symmetric diurnal tidal mode and the symmetric Rossby mode. (The reader should recall that by "mode" we refer to the meridional shape of the forcing—not to the shape of the response.) For purposes of comparison,

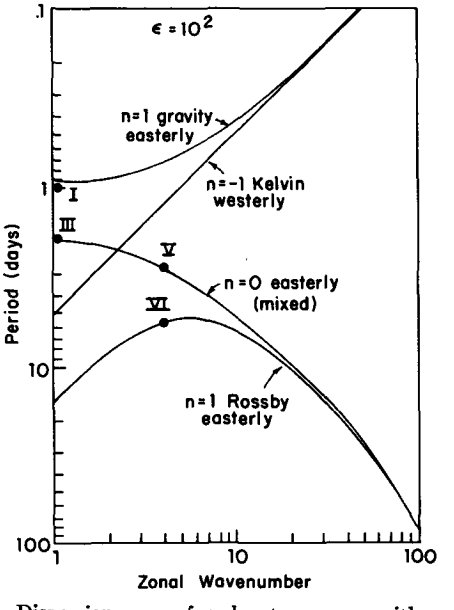

FIG. 1. Dispersion curves for planetary waves with $\epsilon=10^2$. Modes I, III, V and VI (see Table 1) are indicated.

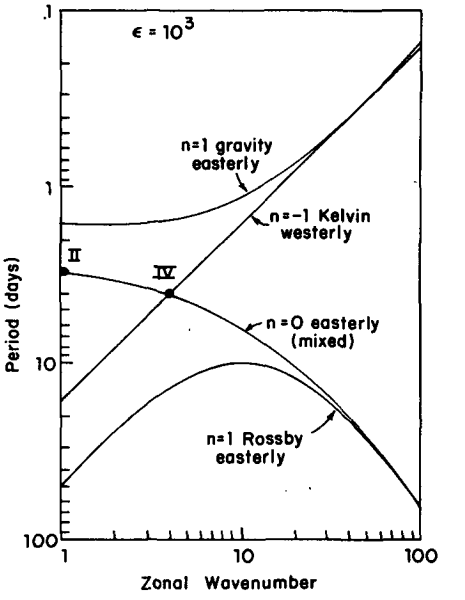

FIG. 2. As in Fig. 1 except $\epsilon=10^3$. Modes II and IV (see Table 1) are indicated.

both viscous and inviscid results are displayed. The following should be noted in connection with these two figures:

1) There is a general tendency for the viscous solutions to approach the inviscid solutions with increasing

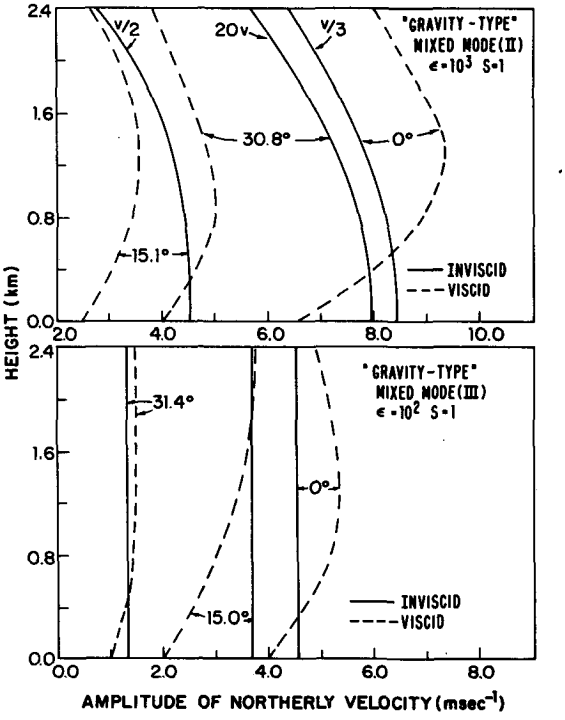

FIG. 3. Amplitude of northerly velocity versus height for inviscid (solid line) and viscid (dashed line) calculations at selected latitudes for mixed Rossby gravity modes II and III.

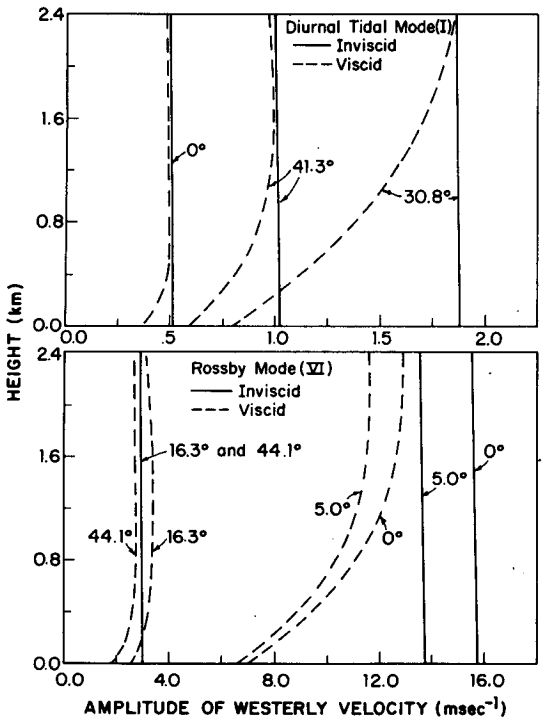

FIG. 4. Amplitude of westerly velocity versus height for inviscid (solid line) and viscid (dashed line) calculations at selected latitudes for diurnal tidal mode I and Rossby mode VI.

height. This tendency is extremely clear for the diurnal tidal mode and somewhat less clear for the other modes. Indeed, there is no *a priori* reason to assume that the two solutions should ever completely coincide. The structure of the inviscid mode depends on the perfect reflection of the mode at the ground; the presence of viscosity certainly alters this condition somewhat. Nevertheless, it turns out (not shown in the figures) the coincidence becomes quite close by 5 km for all modes.

2) On the basis of Figs. 3 and 4 one may subjectively identify a boundary layer thickness marking the transition to inviscid-type behavior. Such a thickness appears to have the following characteristics:

(i) For modes with critical latitudes $\theta_c > 7.5°$ latitude, there is an increase by a factor of 2–3 in this thickness in a 10° latitude neighborhood of θ_c. For critical latitudes closer to the equator, this thickness appears to have its maximum in the neighborhood of the equator. The enhanced thicknesses are modest compared to the infinite thicknesses suggested by Holton *et al.* (1971). Moreover, we do not believe our thicknesses to be significantly "smoothed" by finite differences since our grid separation is small compared to the region over which the increase in thickness takes place.

(ii) As can be seen by comparing the two cases in Fig. 3, this thickness is not significantly dependent on the inviscid vertical wavelength. Rather, it depends primarily on the wave frequency and viscosity equatorward of θ_c (as in a Stokes boundary layer) and primarily on the Coriolis frequency and viscosity poleward of θ_c (as in an Ekman layer).

The situation with respect to vertical velocity is indicated in Fig. 5. For the diurnal tidal mode, which is characteristic of the gravity-wave type solutions, there is no obvious boundary layer character for the w-field. The viscous and inviscid solutions satisfy the same lower boundary condition; there is merely a tendency (with a notable exception to be discussed shortly) for viscosity to diminish w somewhat. For the Rossby mode, on the other hand, there is a marked boundary layer in w associated with Ekman pumping. Interestingly, if we were to have defined boundary layer thickness, in this case, with the height at which the viscous w differs most from the inviscid w we would find that thickness to be relatively independent of latitude.

Since we are primarily concerned with the effect of viscous boundary layers on the low-level convergence field (as manifested by w) we shall study this in greater detail. Figs. 6–10 show the variation with latitude of both the amplitude and phase of w at about 600 m height for both viscous and inviscid calculations of

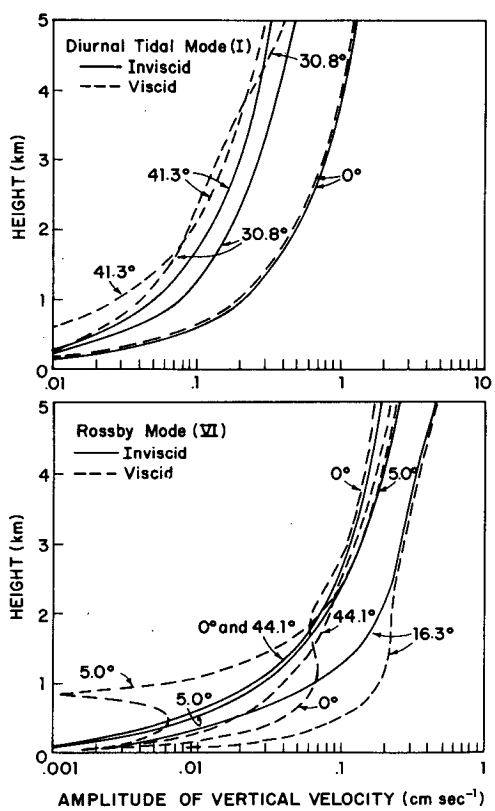

FIG. 5. As in Fig. 4 except for amplitude of vertical velocity.

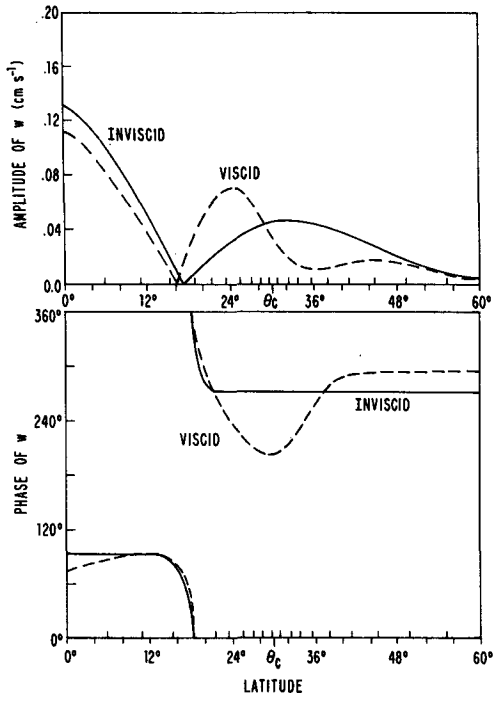

FIG. 6. Amplitude (top) and phase (bottom) of vertical velocity for inviscid (solid line) and viscid (dashed line) calculations for the first symmetric propagating diurnal tidal mode I. Vertical lines on abcissa scale represent grid points used in numerical integration, and the critical latitude (θ_c) is indicated.

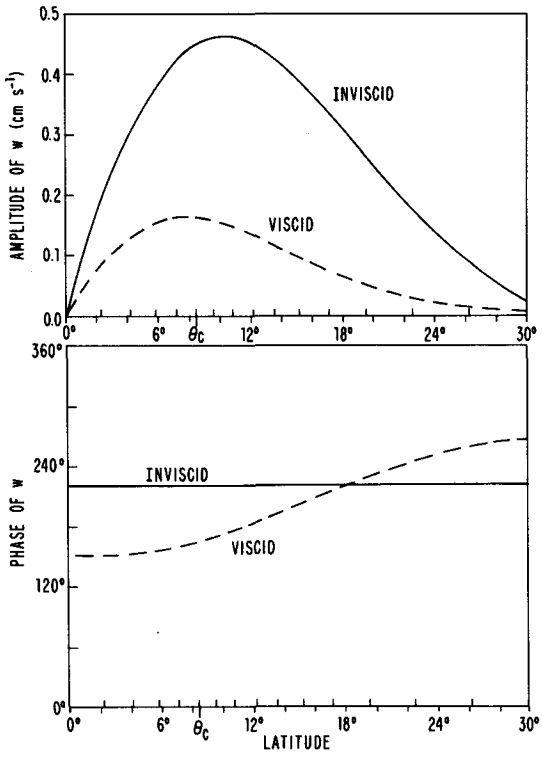

FIG. 7. As in Fig. 6 except for mixed Rossby-gravity mode II with $\epsilon=10^3$, $s=1$ and $T=3.06$ days.

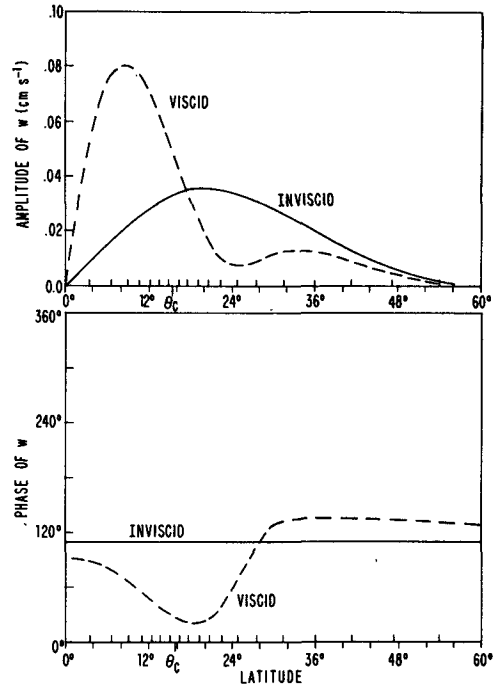

FIG. 8. As in Fig. 6 except for mixed Rossby-gravity mode III with $\epsilon=10^2$, $s=1$ and $T=1.85$ days.

various modes. The following are the main implications we draw from the results in these figures:

1) The gravity mode II with short vertical wavelength has a general reduction of w. Rossby modes V and VI have a general enhancement of w. The gravity modes with long vertical wavelengths, I and III, have more complicated patterns with regions of enhanced and diminished w.

2) There is no indication that w is greatly enhanced at θ_c. For mode V, maximum w, in the viscous case, does occur near θ_c, but this is not the case for any of the other modes.[2]

3) The presence of viscosity causes the phase of w to vary with latitude.

In order to clarify the situation described in item 1 above we have evaluated the projection of the viscous solution for w on the inviscid solution:

$$P(z)=\frac{\int_{-1}^{1} w_{\text{inviscid}} w_{\text{viscous}} d\mu}{\int_{-1}^{1} w_{\text{inviscid}} d\mu}, \tag{18}$$

[2] Hayashi (1971) noted, in connection with simplified calculations where the Ekman depth was forced to be finite, that modes with symmetric pressure fields do not necessarily have maximum w at critical latitudes. The present results show that such a result does not depend on symmetry characteristics. Kuo (1975) has also noted that maximum w is not generally associated with critical latitudes.

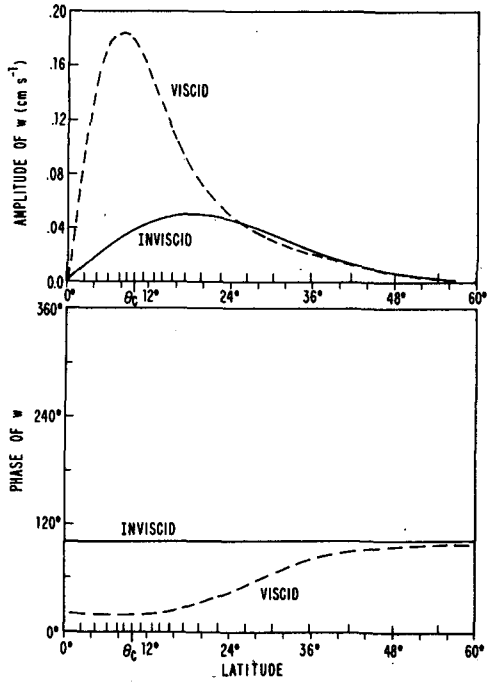

FIG. 9. As in Fig. 6 except for mixed Rossby-gravity mode V with $\epsilon=10^2$, $s=4$ and $T=2.94$ days.

where $\mu=\cos\theta$ and $\theta=$colatitude. Since w_{inviscid} has the meridional structure of a Hough mode, any part of w_{viscous} which does not have a projection on w_{inviscid} is orthogonal to the forced mode. In studying wave CISK, it is that part of w which does have a projection on the inviscid mode that will be of greatest importance. Table 2 gives $P(z)$ for the various modes studied.

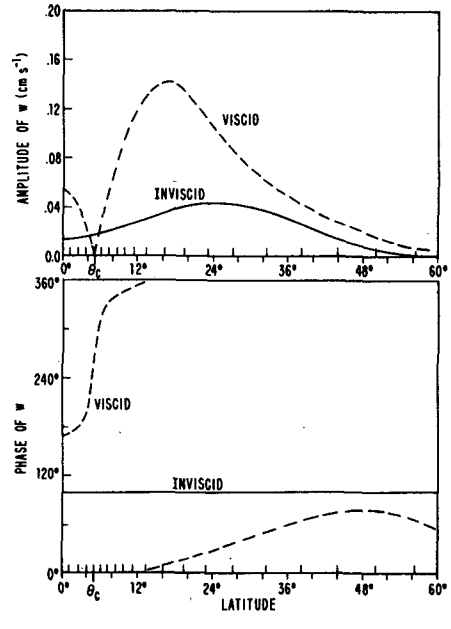

FIG. 10. As in Fig. 6 except for Rossby mode VI with $\epsilon=10^2$, $s=4$ and $T=5.88$ days.

Viewed in this manner there is a clear distinction between gravity and Rossby wave modes. Only the latter give rise to significant low-level boundary layer pumping in the excited mode (though frictional damping diminishes the effect with increasing height). With gravity waves we see that those with relatively short periods and long vertical wavelengths (modes I and III) have projections which differ only slightly from unity; those gravity waves with longer periods and shorter vertical wavelengths (II and IV) suffer significant reduction of low-level convergence in the presence of viscosity.

The apparent enhancement of w in local regions for modes I and III (*viz.*, Figs. 6 and 8) is seen to be entirely due to the generation of modes orthogonal to those directly forced. Such mode coupling is a consequence of the inseparability of the viscous equations [for other examples of such mode coupling, cf. Lindzen and Hong (1974), Hong and Lindzen (1976) and Forbes and Garrett (1976)]. Our tentative conclusion from the few cases we have studied is that mode coupling increases as the ratio of inviscid vertical wave scale (vertical wavelength divided by 2π) to boundary layer scale increases. Moreover, the coupled orthogonal modes tend to have shorter vertical wavelengths and are more subject to damping outside the boundary layer. This last effect is increased as the wave period increases.

Finally, we may recall that in the calculations of Holton *et al.* (1971; see also Lindzen, 1972) it was noted that equatorward of the critical latitude the boundary layer should be similar to a Stokes boundary layer while poleward of θ_c it should be similar to an Ekman layer. An examination of the westerly and northerly velocity fields in our viscous calculations (for purposes of brevity we do not present these results in detail) does show the following features, indicative of such a transition:

1) At a given depth within the boundary layer region (height $\lesssim 1$ km) there is a phase shift ($\sim$90–180°) across the critical latitude θ_c spread over a latitude span of about 15°.

2) Between two given levels within the boundary layer (e.g., 0 and 600 m), the gravity type waves exhibit upward phase progression ($\sim$10° phase km^{-1}) equatorward of θ_c, and downward phase progression ($\sim$10–20° phase km^{-1}) poleward of θ_c. The Rossby-type

TABLE 2. P-values computed from Eq. (18).

Height (km)	I	II	III	IV	V	VI
0.5	0.85	0.33	1.17	0.21	6.13	3.60
1.0	0.87	0.35	1.04	0.21	2.51	1.70
1.5	0.90	0.36	0.94	0.20	1.97	1.30
2.0	0.91	0.36	0.90	0.19	1.61	1.04
2.5	0.91	0.36	0.87	0.19	1.34	0.90

waves exhibit a similar transition 5–10° poleward of the critical latitude.

6. Conclusions

As already has been noted, computational economy has prevented us from carrying out a complete study of the boundary layers produced by thermally forced waves in a rotating, spherical atmosphere. Nevertheless, the limited number of cases studied do permit some reasonably firm conclusions. Most significant, perhaps, is a negative finding, namely, *no* special boundary layer convergence is found at critical latitudes. As noted in the Introduction, the projection of the wave response on the forced mode has enhanced boundary layer convergence only for Rossby-type modes and the enhanced convergence is due essentially to Ekman pumping. In view of the above, it should prove generally adequate to model spherical Rossby waves with their counterparts on a midlatitude β-plane—at least with respect to boundary layer processes. This approach has been followed by Shapiro (1977) and Stevens and Lindzen (1978).

For gravity waves, we have shown that significantly enhanced boundary layer convergence occurs only due to the generation of modes orthogonal to the forced mode. To the extent that such modes are of interest, simple separable approximations to the present spherical model will be inadequate. However, in many cases the projection of the response on the forced mode is of primary interest and in such cases, simpler models should again be adequate.

Acknowledgment. The authors wish to acknowledge the support of the National Science Foundation through Grant ATM-75-20156.

REFERENCES

Chapman, S., and R. S. Lindzen, 1970: *Atmospheric Tides*. Reidel, 200 pp.

Charney, J. G., 1971: Tropical cyclogenesis and the formation of the intertropical convergence zone. *Lectures in Applied Mathematics*, Vol. 13, Amer. Math. Soc., 355–368.

——, and A. Eliassen, 1964: On the growth of the hurricane depression. *J. Atmos. Sci.*, **21**, 68–75.

Forbes, J. M., and H. B. Garrett, 1976: Solar diurnal tide in the thermosphere. *J. Atmos. Sci.*, **33**, 2226–2241.

Greenspan, H. P., 1968: *The Theory of Rotating Fluids*. Cambridge University Press, 327 pp.

Hayashi, Y., 1970: A theory of large-scale equatorial waves generated by condensation heat and accelerating the zonal wind. *J. Meteor. Soc. Japan*, **48**, 140–160.

——, 1971: Frictional convergence due to large-scale equatorial waves in a finite-depth Ekman layer. *J. Meteor. Soc. Japan*, **49**, 450–457.

Holton, J. R., 1975: On the influence of boundary layer friction on mixed Rossby-gravity waves. *Tellus*, **27**, 107–115.

——, J. M. Wallace and J. Young, 1971: On boundary layer dynamics and the ITCZ. *J. Atmos. Sci.*, **28**, 275–280.

Hong, S. S., and R. S. Lindzen, 1976: Solar semidiurnal tide in the thermosphere. *J. Atmos. Sci.*, **33**, 135–153.

Kuo, H. L., 1973: Planetary boundary layer flow of a stable atmosphere over the globe. *J. Atmos. Sci.*, **30**, 53–65.

——, 1975: Planetary boundary layer of equatorial waves and critical latitude. *Bound.-Layer Meteor.*, **9**, 163–190.

Lindzen, R. S., 1970: Internal gravity waves in atmospheres with realistic dissipation and temperature. Part I. Mathematical development and propagation of waves into the thermosphere. *Geophys. Fluid Dyn.*, **1**, 303–355.

——, 1972: Lectures on tropical meteorology. *Dynamics of the Tropical Atmosphere*, John Young, Ed., *Proc. NCAR Summer Colloquium*, 107–182.

——, 1974: Wave-CISK in the tropics. *J. Atmos. Sci.*, **31**, 156–179.

——, and S. S. Hong, 1974: Effects of mean winds and horizontal temperature gradients on solar and lunar semidiurnal tides in the atmosphere. *J. Atmos. Sci.*, **31**, 1421–1446.

——, and H. L. Kuo, 1969: A reliable method for the numerical integration of a large class of ordinary and partial differential equations. *Mon. Wea. Rev.*, **97**, 732–734.

Longuet-Higgins, M. S., 1968: The eigenfunctions of Laplace's tidal equations over a sphere. *Phil. Trans. Roy. Soc. London*, **A262**, 511–607.

Schneider, E. K., and R. S. Lindzen, 1976: The influence of stable stratification on the thermally driven tropical boundary layer. *J. Atmos. Sci.*, **33**, 1301–1307.

Shapiro, L. J., 1977: Frictional effects on thermally forced waves. *Tellus*, **29**, 264–271.

Stevens, D., and R. S. Lindzen, 1978: Tropical Wave-CISK with a moisture budget and cumulus friction. Submitted to *J. Atmos. Sci.*

Yamasaki, M., 1971: Frictional convergence in Rossby waves in low latitudes. *J. Meteor. Soc. Japan*, **49** (Syono Memorial Volume), 691–698.